

Subretinal Rather Than Intravitreal Adeno-Associated Virus–Mediated Delivery of a Complement Alternative Pathway Inhibitor Is Effective in a Mouse Model of RPE Damage

Balasubramaniam Annamalai,¹ Nathaniel Parsons,¹ Crystal Nicholson,¹ Elisabeth Obert,¹ Bryan Jones,² and Bärbel Rohrer^{1,3,4}

¹Department of Ophthalmology, Medical University of South Carolina, Charleston, South Carolina, United States

²Department of Ophthalmology, University of Utah, Salt Lake City, Utah, United States

³Division of Research, Ralph H. Johnson VA Medical Center, Charleston, South Carolina, United States

⁴Department of Neurosciences, Medical University of South Carolina, Charleston, South Carolina, United States

Correspondence: Bärbel Rohrer, Department of Ophthalmology, Medical University of South Carolina, 167 Ashley Avenue, Charleston, SC 29425, USA; rohrer@musc.edu.

BA and NP contributed equally to the manuscript.

Received: February 12, 2021

Accepted: March 4, 2021

Published: April 8, 2021

Citation: Annamalai B, Parsons N, Nicholson C, Obert E, Jones B, Rohrer B. Subretinal rather than intravitreal adeno-associated virus–mediated delivery of a complement alternative pathway inhibitor is effective in a mouse model of RPE damage. *Invest Ophthalmol Vis Sci.* 2021;62(4):11. <https://doi.org/10.1167/iovs.62.4.11>

PURPOSE. The risk for age-related macular degeneration has been tied to an overactive complement system. Despite combined attempts by academia and industry to develop therapeutics that modulate the complement response, particularly in the late geographic atrophy form of advanced AMD, to date, there is no effective treatment. We have previously demonstrated that pathology in the smoke-induced ocular pathology (SIOP) model, a model with similarities to dry AMD, is dependent on activation of the alternative complement pathway and that a novel complement activation site targeted inhibitor of the alternative pathway can be delivered to ocular tissues via an adeno-associated virus (AAV).

METHODS. Two different viral vectors for specific tissue targeting were compared: AAV5-VMD2-CR2-fH for delivery to the retinal pigment epithelium (RPE) and AAV2YF-smCBA-CR2-fH for delivery to retinal ganglion cells (RGCs). Efficacy was tested in SIOP (6 months of passive smoke inhalation), assessing visual function (optokinetic responses), retinal structure (optical coherence tomography), and integrity of the RPE and Bruch's membrane (electron microscopy). Protein chemistry was used to assess complement activation, CR2-fH tissue distribution, and CR2-fH transport across the RPE.

RESULTS. RPE- but not RGC-mediated secretion of CR2-fH was found to reduce SIOP and complement activation in RPE/choroid. Bioavailability of CR2-fH in RPE/choroid could be confirmed only after AAV5-VMD2-CR2-fH treatment, and inefficient, adenosine triphosphate–dependent transport of CR2-fH across the RPE was identified.

CONCLUSIONS. Our results suggest that complement inhibition for AMD-like pathology is required basal to the RPE and argues in favor of AAV vector delivery to the RPE or outside the blood-retina barrier.

Keywords: complement system, choroidal neovascularization, smoke-induced ocular pathology, natural antibody-mediated targeting, alternative pathway inhibitor, encapsulated ARPE-19 cells

Age-related macular degeneration (AMD) is a slowly progressing neurodegenerative disease leading to loss of vision in the center of the field of vision. In dry AMD, which makes up 80% to 90% of total cases, this loss of vision appears to start with pathology in the retinal pigment epithelium (RPE) and the choriocapillaris, followed by the slow degeneration and atrophy of the photoreceptors in the macula.¹ The changes in the RPE/choroid interface include thickening of Bruch's membrane,² thinning of the choriocapillaris and loss of fenestrations,³ mitochondrial damage and dysfunction,⁴ and a deterioration of the blood-retina barrier.⁵ Finally, complement dysregulation in those tissues appears to contribute to the pathology.⁶

The complement system is an essential part of the innate and adaptive immune system, and studies in experimental inflammatory injuries have taught us that the complement system plays a pivotal role in induction and expansion of injury.^{7,8} The complement system is activated by three pathways: the classical pathway, the lectin pathway, and the alternative pathway (AP), which generate a cascade of convertases belonging to a family of serine proteases, the C3 and C5 convertases. Their sequential activation leads to the production of biological effector molecules, the anaphylatoxins C3a and C5a, which activate and recruit immune cells, the opsonins, which are C3 fragments that covalently bind to cells and debris to facilitate their removal by immune

cells, and the membrane attack complex (MAC), a nonspecific pore that can lead to lysis of nonself cells.⁹ The AP is the most potent driver of AMD pathology in patients and their animal models.^{10,11} In order to prevent excessive AP complement activation, the system relies on the available cell-bound and soluble inhibitors. Complement factor H (fH) can inhibit the formation of the C3 convertase and accelerate its decay and cleavage, whereas the complement receptor 1 and decay accelerating factor (DAF/CD55) prevent the assembly of the C3 convertase on the cell surface.¹² Given its importance as a complement regulator, fH is present in human and rodent serum at a high concentration (300–600 µg/mL), and single-nucleotide polymorphisms in fH pose risks for AMD.¹³

Based on the genetics of AMD, some of the major efforts in the development of new therapeutics have been focused on complement inhibitors. Approaches have included blocking complement components C3 and C5 (activators in the common terminal pathway) or factor D (fD; AP activator), using either humanized monoclonal antibodies (eculizumab [intravenous injection] and LFG316 [intravitreal]) or their FAB fragments (lampalizumab [intravitreal]), RNA aptamers (ARC-1905 [intravitreal]), or synthetic cyclic peptide (APL-2 [intravitreal]). The three trials targeting C5 did not decrease the growth rate of GA significantly,¹⁴ or the studies were completed but results were not published (summarized in Taskintuna et al.¹⁵). Despite having achieved significance in a subgroup of patients with dry AMD with complement factor I (CFI) risk variants treated with lampalizumab phase II trial known as MAHALO, NCT01229215 in 2014,¹⁶ the phase III clinical trials ultimately did not reach their clinical endpoint.¹⁷ Three molecules are currently under investigation for all patients with GA, a pegylated peptide form of APL-2, a pegylated anti-C5 aptamer, and soluble CD59 (a MAC inhibitor),¹⁸ and two approaches are tailored toward patients with loss-of-function variants in complement factor H (CFH) (NCT04643886) and CFI (NCT04437368). We argue, based on these results, that the target (reducing complement activation) is the correct one, but in most trials, the drug and the delivery were insufficient. As the complement system is a surveillance system, most of the complement proteins are not engaged in active complement activation, suggesting that most of the drug is wasted on target molecules that are irrelevant to pathophysiology. The second complication is that complement components are made in the eye and the liver and that some select complement components can penetrate the Bruch's membrane (BrM) to reach the basal side of the RPE, whereas others do not, creating different complement compartments.¹⁹ And third, if the targets of complement activation in dry AMD are the basal side of the RPE, BrM, and choriocapillaris (CC), as suggested by the distribution of complement activation products in diseased eyes,^{20,21} intravitreal injections might not be appropriate for drug delivery due to the barrier function of the external/outer limiting membrane²² and the RPE.²³

We previously characterized an AP complement inhibitor molecule that enables specific targeting to tissues under complement attack. CR2-fH is a fusion protein that consists of short consensus repeats (SCRs) 1 to 5 of mouse fH (the domain required for its regulatory activity) linked to the portion of the complement receptor 2 (CR2) that binds C3-based opsonins.²⁴ And while CR2-based inhibitors have a circulatory half-life of ~9 hours, their half-life in injured tissues is ~50 hours.²⁵ Efficacy and targeting to sites of complement activation have been confirmed in AMD models both *in vitro*^{26,27} and in two *in vivo* models, the laser-

induced choroidal neovascularization (CNV) model, a model for VEGF- and complement-dependent angiogenesis,^{28,29} and the smoke-induced ocular pathology (SIOP), a model for oxidative and complement stress-mediated RPE, Bruch's membrane, and choriocapillaris damage.³⁰ Therapeutic efficacy could be demonstrated when applied systemically as soluble protein,^{31,32} administered intraocularly or systemically using encapsulated ARPE-19 cells producing CR2-fH,^{33,34} and using gene therapy.³⁵ CR2-fH gene therapy was tested using AAV5-VMD2-CR2-fH for delivery to RPE in the mouse laser-induced CNV model and was considered safe based on lack of anti-CR2-fH antibody production, effects on structure, and function of the retina and the RPE.³⁵

Here we investigate the placement of the therapeutics for its optimal effect in the SIOP model; in other words, will CR2-fH reach the tissue of complement activation optimally when placed subretinally, or can intravitreal delivery be employed?

METHODS

Adeno-Associated Virus Constructs

The plasmid construct of CR2-fH³¹ and the adeno-associated virus 2/5 (AAV5) construct³⁵ were previously described. In short, CR2-fH is assembled based on the four *N*-terminal SCRs of mouse CR2 (residues 1–257, accession number M35684) followed by a (G₄S)₂ linker and the five *N*-terminal SCRs of mouse fH (residues 1–303, accession number NM009888). To ensure secretion, a CD5 signal peptide sequence was added,³⁶ and protein secretion into the apical and basal compartment in polarized, infected RPE cells was confirmed.³⁵ Two vector backbones, AAV5³⁵ and AAV2YF,³⁷ were utilized based on their ability to transduce RPE³⁸ and retinal ganglion cells (RGCs) and secondary neurons (together referred to as inner retinal cells),^{39,40} respectively. Likewise, an RPE-specific promoter VMD2 (BEST1) and a generic promoter smCBA were utilized to drive efficient expression. The following three vectors were produced at the Ophthalmology Vector Core at the University of Florida: AAV5-VMD2-CR2-fH, AAV2YF-smCBA-CR2-fH, and AAV5-VMD2-mCherry.

Mice

C57BL/6J (B6) mice were generated from breeding pairs (Jackson Laboratory, Bar Harbor, ME, USA) to obtain mice always raised within the same microenvironment. Mice entered the study at 2 months of age, and both sexes were included. All animal experiments were performed in accordance with the ARVO Statement for the Use of Animals in Ophthalmic and Vision Research and approved by the University Animal Care and Use Committee.

Viral Vector Injection

Subretinal and intravitreal injections were performed using the trans-cornea route according to our published protocol.³⁵ In short, mice were anesthetized using xylazine and ketamine (20 and 80 mg/kg, respectively), both pupils dilated (phenylephrine HCL, 2.5%, and atropine sulfate, 1%), and the ocular surface anesthetized (proparacaine hydrochloride) and lubricated (hydroxypropyl methylcellulose, 2.5%). Injections were made through a guide hole

generated in the superior cornea (30 $\frac{1}{2}$ -gauge disposal needle) using a 33-gauge unbeveled blunt needle affixed to a Hamilton syringe (2.5 μ L; Hamilton Co., Reno, NV, USA) into the vitreous (intravitreal delivery) or the subretinal space (subretinal delivery). Then, 1 μ L of vector suspension was slowly injected into both eyes of each animal. For subretinal injections, subretinal blebs formation is an indication of success, and retinal detachment was confirmed by optical coherence tomography (OCT) and fundus photography to document size and location. For subretinal injections, a concentration of 3×10^{11} viral genomes (vg)/mL AAV5-VMD2-CR2-fH was found to be both efficacious and safe.³⁵ In preliminary experiments for intravitreal delivery, viral concentrations ranging from 1 μ L of 1×10^{15} vg containing particles/mL (AAV2-smCBA-CR2-fH) to 1 μ L of 1×10^{10} vg/mL were tested. A safe dose was considered the number of vg/mL that produced the same number of infiltrating cells on OCT when compared to a 1- μ L injection with PBS in the absence of oral steroid prophylaxis. A concentration of 3×10^{11} vg/mL AAV2-smCBA-CR2-fH was found to be safe.

Exposure to Cigarette Smoke

One month following the adeno-associated virus (AAV) delivery, mice were subjected to cigarette smoke exposure (CSE) over a period of 6 months as published previously.³⁰ Smoke exposure was carried out by burning 3R4F reference cigarettes (University of Kentucky, Louisville, KY, USA) using a smoking machine (Model TE-10; Teague Enterprises, Woodland, CA, USA) for 5 hours per day, 5 days per week.

Optical Coherence Tomography

OCT was used to quantify retinal thickness as described in detail.³⁰ In short, imaging was performed using an SD-OCT Bioptigen Spectral Domain Ophthalmic Imaging System (Bioptigen, Inc., Durham, NC, USA), collecting five separate rectangular volume scans (33 B-scans, 1000 A-scans per B-scan) that were averaged to obtain a high-resolution image. Measurements were obtained 500 μ m from the optic disc in the nasal quadrant using calibrated vertical calipers.³⁰

Optokinetic Response Test

Visual acuity and contrast sensitivity of mice were measured using the OptoMotry device (Cerebral Mechanics, Lethbridge, Alberta, Canada) as previously described.³⁰ In short, optomotor responses are assessed under photopic conditions (mean luminance of 52 cd m⁻²), utilizing to moving sine-wave gratings. Two threshold responses were obtained: visual acuity characterized as the spatial frequency threshold of each animal (at a speed of 12 deg/s and 100% contrast) and contrast sensitivity threshold (at a fixed spatial frequency of 0.131 cyc/deg and 12 deg/s speed).

Electron Microscopy

Tissue preparation and ultrastructural analyses were performed as previously described.^{32,41} Transmission electron microscopy images were captured using a JEOL JEM 1400 transmission electron microscope (JEOL USA, Inc., Peabody MA, USA) using SerialEM software (<https://bio3d.colorado.edu/SerialEM/>). The resulting data sets (1200–1500 images per section) were assembled into mosaics using the NCR Toolset (Scientific Computing and Imaging Insti-

tute, Salt Lake City, UT, USA).^{42,43} Structures were evaluated using Adobe Photoshop (Adobe Systems, San Jose, CA, USA) and ImageJ software (National Institutes of Health, Bethesda, MD, USA) as published previously.³⁰ BrM thickness was determined by analyzing a ~ 24 - μ m length section of BrM per sample. BrM thickness in age-matched room air-exposed mice was consistently 0.22 ± 0.04 μ m, and a thickness exceeding 0.28 μ m was considered damaged.⁴¹ The percentage of thickened BrM was assessed. Each stretch of thickened BrM was called a deposit (see Fig. 3A), and for those, their length and area were assessed. In addition, mitochondria in the RPE were identified, outlined, and evaluated for morphologies indicating pathology using ImageJ's shape descriptor "circularity." Mitochondria normally assume elongated shapes. When form factors shift toward 1 (circular),⁴⁴ this indicates mitochondrial swelling and resultant pathologies.

Dot Blot and Western Analysis

To quantify complement activation in the eye, RPE/choroid samples were collected, protein extracted, separated by electrophoresis, and transferred to a Polyvinylidene Difluoride (PVDF) membrane, and membranes were incubated with primary antibody against C3d generated by us⁴⁵ as published previously.⁴¹ This antibody (group 2, clone 11) recognizes the C3d epitope present in the C3 α chain and its breakdown fragments, which can be distinguished according to their molecular weights.⁴⁵ Due to the similar molecular weights of C3dg (39 kD) and C3d (34 kD), the two bands separate poorly and are evaluated together. To assess leakage of the outer retina barrier, the amount of albumin (Novus Biologicals, Littleton, CO, USA) present in the retina was assessed. Proteins were visualized with horseradish peroxidase-conjugated secondary antibodies (Santa Cruz Biotechnology, Dallas, TX, USA) followed by incubation with Clarity Western ECL Blotting Substrate (Bio-Rad, Hercules, CA, USA) and chemiluminescent detection. Blots representing the different experimental groups were all exposed together for the same length of time to allow for comparison. Band intensities were determined using ImageJ and normalized against β -actin.

To determine the amount of CR2-fH in the retina, RPE/choroid, or ARPE-19 cell supernatants, protein samples or apical and basal supernatants were collected, loaded directly into the wells of a 96-well plate, and transferred onto nitrocellulose membranes using the Bio-Dot Microfiltration Apparatus (Bio-Rad Laboratories, Inc., Hercules, CA, USA) as reported previously.³⁵ CR2-fH was detected using an anti-CR2 primary antibody (10 μ g/mL; rat anti-mouse CD21, clone 7G6; purified in-house³⁶) and visualized as described for Western blotting.

ARPE-19 Cell Cultures

ARPE-19 cells, a human RPE cell line, were expanded and developed into monolayers as previously described.⁴⁶ These cells generate a polarized RPE cell monolayer when plated on Transwell filters (Corning #3450, Fisher Scientific, Waltham, MA, USA) with robust RPE barrier properties afforded by tight junctions and characterized by minimal apical to basolateral movement of [carboxy-¹⁴C]-inulin.⁴⁷ A dose of 10 μ g/mL humanized CR2-fH was added to the apical side, and supernatants (apical and basal) were collected for analysis after 4 hours. Adenosine triphosphate

(ATP)-dependent transport was assessed after pretreatment with 30 mM NaN_3 , a mitochondrial inhibitor.⁴⁸

Data Analysis and Statistics

Data are presented as mean \pm SEM. Single comparisons were analyzed using unpaired *t*-tests. Data consisting of multiple groups were analyzed by ANOVA (with Bonferroni correction for multiple comparison), with mean value differences considered significant at $P \leq 0.05$ (StatView; SAS Institute, Inc., Cary, NC, USA).

RESULTS

Subretinal Delivery of AAV5-VMD2-CR2-fH Reduces SIOP

Secondhand smoke exposure for 6 months in mice leads to pathology in the RPE that is dependent on the activation of the AP of complement.³⁰ Those alterations include a thickening of BrM and swelling of mitochondria as well as lipid accumulation,⁴⁹ leading to loss of contrast sensitivity in the optokinetic response (OKR) and reduction in ERG amplitudes.³⁰ Previously, we have shown that treatment with the AP inhibitor CR2-fH after 6 months of smoke restored contrast sensitivity in the mice as well as allowed for the repair of the RPE/BrM/choroid complex.³² Based on these observations, we tested the effectiveness of AAV5-VMD2-CR2-fH to prevent SIOP when delivered subretinally. In previously published experiments, the equivalent effective concentration of subretinally injected AAV5-VMD2-CR2-fH when compared to intravenously delivered protein³¹ to reduce CNV progression was determined to be 3×10^{11} vg/mL.³⁵ Since the same amount of intravenously delivered protein used for CNV is efficacious in SIOP, a dose of 3×10^{11} vg/mL was used for the SIOP experiments here.

AAV5-VMD2-CR2-fH or AAV5-VMD2-mCherry was delivered subretinally in 2-month-old mice. One month later, which is sufficient time for the retina to reattach and the retinal response to return to baseline,³⁵ half the animals were exposed to long-term smoke inhalation as reported previously, and the rest remained in room air.³⁰ After the completion of the 6-month smoke exposure period, optokinetic responses were assessed to determine visual function. As reported previously, spatial acuity in C57BL/6J mice was not affected by CSE as compared to room air exposure (Fig. 1A) or by the gene therapy, with all four groups having indistinguishable spatial acuity. However, contrast threshold (percent contrast required to elicit a response) was elevated in CSE mice treated with mCherry, which exhibited a significant increase in contrast threshold compared to never-smokers (mCherry: 26.6 ± 3.5 vs. mCherry never-smokers: 12.3 ± 1.16 ; $P < 0.0001$; Fig. 1B). Contrast thresholds in CSE mice treated with CR2-fH were significantly improved when compared to those treated with mCherry (smoke + CR2-fH: 18.6 ± 1.99 ; mCherry versus CR2-fH: $P < 0.003$; Fig. 1B) and more similar to those of CR2-fH age-matched never-smokers (smoke + CR2-fH: 18.6 ± 1.99 ; room air + CR2-fH: 14.0 ± 2.00 ; Fig. 1B).

The structural alterations associated with SIOP^{30,32,41} were assessed in the four groups of animals. SD-OCT analysis, analyzing total retinal thickness, identified a smoke effect (room air versus smoke: $P < 0.001$) but no treatment effect (CR2-fH versus mCherry: room air, $P = 0.86$; smoke, $P = 0.43$) (Fig. 2). We used transmission electron micro-

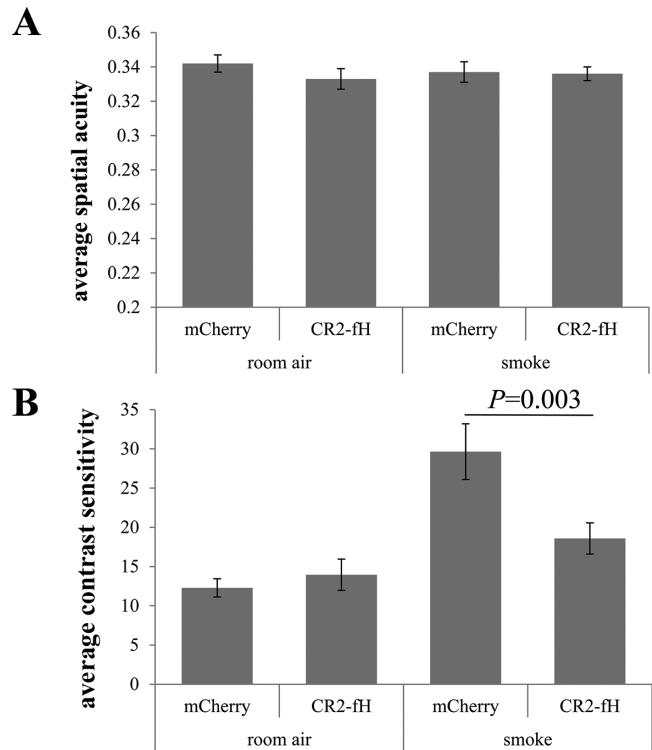


FIGURE 1. Effects of subretinal CR2-fH delivery on visual function in the SIOP model. Animals were injected at 2 months of age with AAV5-VMD2 vectors expressing mCherry or CR2-fH, followed by 6 months of smoke or room air exposure. After completion of the study, animals were tested for spatial acuity and contrast threshold using the Optomotry device. (A) Spatial acuity, as assessed at 100% contrast, was not affected by smoke or treatment. (B) Contrast threshold was determined at a fixed spatial frequency (0.131 cyc/deg) and speed (12 deg/s). Smoke-exposed mice showed a significant reduction in contrast sensitivity or an increase in threshold compared to controls exposed to room air, which was prevented in mice treated with CR2-fH when compared to mCherry. Data are expressed as mean \pm SEM ($n = 4-6$ eyes per condition).

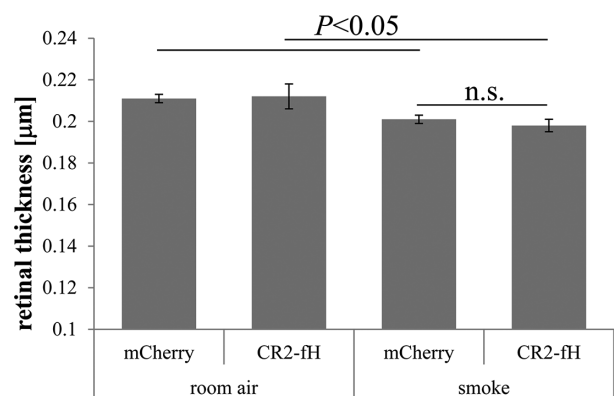


FIGURE 2. Effects of smoke and subretinal CR2-fH delivery on retinal thickness. Overall retinal thickness was assessed by optical coherence tomography. While overall retinal thickness was reduced in response to smoke, this effect could not be ameliorated by gene therapy. Data are expressed as mean \pm SEM ($n = 4-6$ eyes per condition).

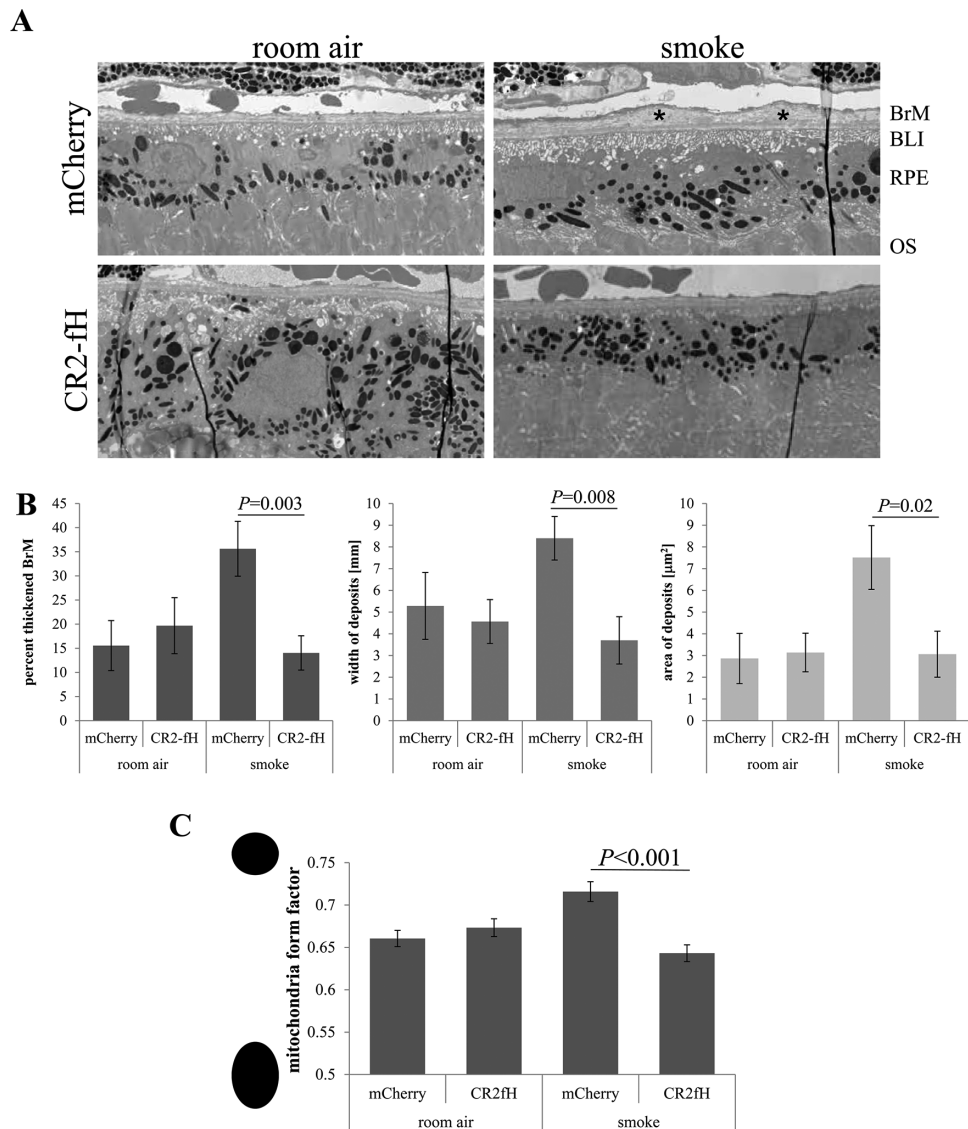


FIGURE 3. Effects of smoke and subretinal CR2-fH delivery on BrM thickness and deposits and mitochondrial swelling. **(A)** Transmission electron micrographs of the RPE obtained from C57BL/6J mice exposed to 6 months of room air or smoke in mCherry- and CR2-fH-treated animals. The BrM in animals exposed to smoke exhibited pathologic changes, including a thickening or deposit formation in BrM. Two deposits are indicated (*). BLI, basolaminarinfoldings; OS, outer segments. **(B)** BrM thickness (*left graph*) was examined and the percent BrM along a given RPE cell that was damaged (exceeds the normal thickness [$>0.28 \mu\text{m}$]⁴¹ of BrM in age-matched room air-exposed mice), and a smoke exposure and treatment effect are demonstrated. Width of the deposits (*middle graph*) and area of the deposits (*right graph*) were likewise increased by smoke and reduced by CR2-fH. **(C)** Mitochondrial swelling in RPE cells was assessed using form factor analysis, with swollen mitochondria becoming more round. Swelling is documented upon smoke exposure, and a treatment effect is demonstrated. Data are expressed as mean \pm SEM ($n = 4\text{--}6$ eyes per condition).

graphs obtained from SIOP animals treated with CR2-fH, mCherry, and age-matched virus-injected never-smokers to compare morphologic alterations in BrM (Fig. 3A). Smoke-exposed mCherry-treated animals exhibited deposits in the outer collagenous layer described by us previously,³⁰ resulting in thickened BrM. The extent of thickened BrM increased with smoke exposure, such that the percent thickened BrM ($>0.28 \mu\text{m}$) increased to $\sim 40\%$ in smoke-exposed mice treated with mCherry, compared to $\sim 14\%$ in smoke-exposed mice treated with CR2-fH (Fig. 3B) ($P < 0.005$). Age-matched never-smoked mice had a small amount of thickened BrM (mCherry versus CR2-fH: $P = 0.54$). Each stretch of thickened BrM ($>0.28 \mu\text{m}$) was called a deposit, which was char-

acterized based on width (in μm ; smoke mCherry: 8.4 ± 1.00 versus smoke CR2-fH: 3.7 ± 1.09 ; $P = 0.007$) and area (in μm^2 ; smoke mCherry: 7.5 ± 1.47 versus smoke CR2-fH: 3.06 ± 1.06 ; $P = 0.02$). CR2-fH reduced these values to baseline levels (width for CR2-fH, room air: 4.57 ± 1.01 versus smoke: 3.7 ± 1.09 ; $P = 0.57$ and area of deposits for CR2-fH, room air: 3.14 ± 0.89 versus smoke: 3.06 ± 1.06 ; $P = 0.96$). Finally, the shape of the mitochondria in the RPE cells in response to treatment was assessed using form factor analysis in ImageJ. A form factor closer to 1 is associated with mitochondrial swelling.⁴⁴ CSE resulted in rounder mitochondria in mCherry-treated animals (room air mCherry versus smoke Cherry: $P < 0.0001$), whereas

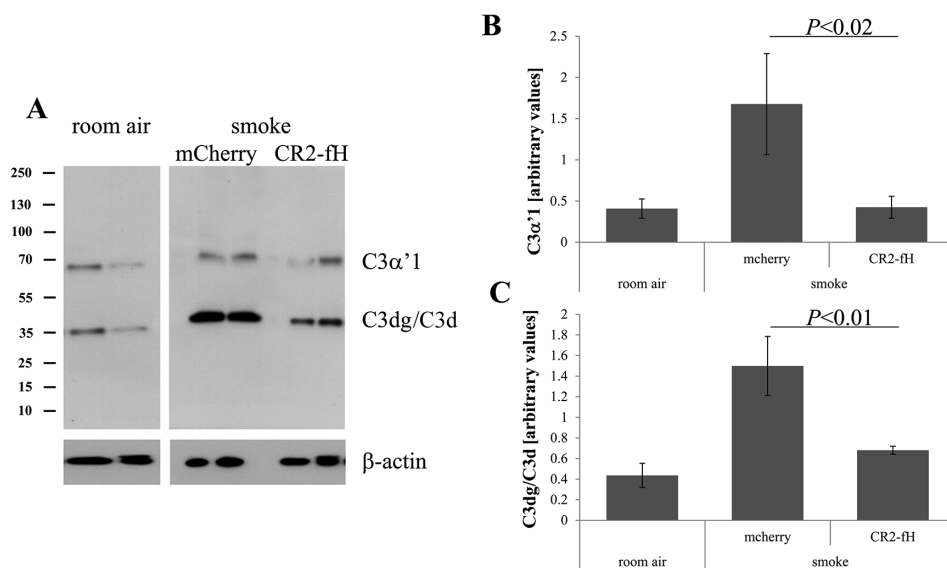


FIGURE 4. RPE-mediated expression CR2-fH reduces complement activation in RPE/choroid. **(A)** Western blot band analysis of complement activation in RPE/choroid extracts (15 μ g/lane) probed for with an antibody against C3d, which recognizes the C3d epitope in C3 α and its breakdown products. Band intensities were quantified and normalized with β -actin. Breakdown products of C3 α were identified according to molecular weight (MW). Biological replicates are presented. **(B)** C3 α '1 and **(C)** C3dg/C3d were significantly elevated in smoke-exposed mCherry-treated mice, whereas CR2-fH-treated mice had levels that were indistinguishable from room air-exposed controls. Data are expressed as mean \pm SEM ($n = 4$ –5 independent samples per condition for protein analysis).

CR2-fH protected against this change (smoke mCherry versus smoke CR2-fH: $P < 0.0001$) with room air CR2-fH compared to smoke CR2-fH-treated animals being indistinguishable ($P = 0.04$).

The level of complement activation products in the RPE/choroid fractions was assessed by Western blotting. Smoke-exposed CR2-fH-injected mice had significantly lower levels of C3 α '1 ($P < 0.02$) and C3dg/C3d ($P < 0.01$) present in the RPE/choroid fraction (Fig. 4) when compared to mCherry-treated mice, with levels indistinguishable to those obtained from animals raised in room air.

Intravitreal Delivery of AAV2-smCBA-CR2-fH Does Not Reduce SIOP

Subretinal injections in patients might not be feasible for a large population with dry AMD, and it is still not clear whether subretinal delivery would protect the entire macular region. Hence, here we tested whether intravitreally delivered AAV2-smCBA-CR2-fH would express sufficient amounts of product in the inner retina to reach the RPE-BrM-choroid area in a mouse. A dose of 3×10^{11} vg/mL was used for the intravitreal delivery based on a comparable immune response between this dose and PBS.

AAV2-smCBA-CR2-fH or PBS was delivered intravitreally in 2-month-old mice followed by exposure to long-term smoke inhalation.³⁰ A no-injection control exposed to smoke and a group of room air-exposed mice was included. After the completion of the 6-month smoke exposure period, optokinetic responses were assessed to determine visual function as for the subretinal delivery group. As spatial acuity in C57BL/6J mice is not affected by smoke exposure (Fig. 1A), only contrast threshold was assessed. Contrast threshold was elevated approximately twofold in CSE mice treated irrespective of treatment ($P < 0.05$) (Fig. 5).

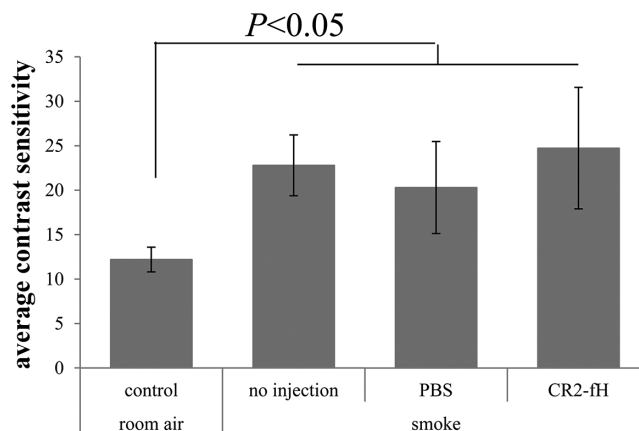


FIGURE 5. Effects of intravitreal CR2-fH delivery on visual function in the SIOP model. Animals were injected at 2 months of age with AAV2-smCBA-CR2-fH vector or PBS or received no injection, followed by 6 months of smoke or room air exposure. After completion of the exposure period, animals were tested as described in Figure 1. Contrast sensitivity as measured by contrast threshold revealed that all smoke-exposed mice, irrespective of treatment, showed a significant elevation of threshold compared to controls exposed to room air. Data are expressed as mean \pm SEM ($n = 4$ –6 eyes per condition).

Electron microscopy analysis of the structure of the outer retina was not performed, due to the lack of an effect on the function of the retina. Assessment of the level of complement activation products in the RPE/choroid fractions suggests that minimal amounts of CR2-fH were delivered to the target tissue to reduce complement activation. When compared to PBS-injected mice, C3 α '1 ($P < 0.05$) and C3dg/C3d ($P < 0.1$) levels present in the RPE/choroid fraction (Figs. 6A–C) were marginally reduced by the presence of CR2-fH.

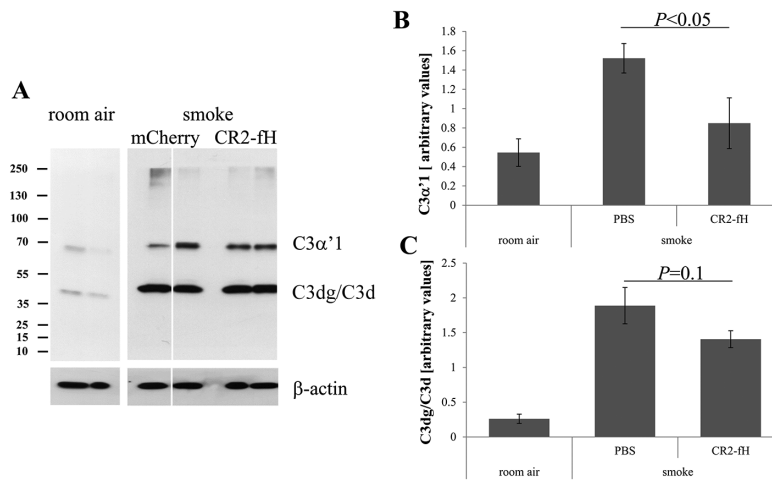


FIGURE 6. RGC-mediated expression CR2-fH has minimal effect on complement activation in RPE/choroid. **(A)** Western blot band analysis of complement activation in RPE/choroid extracts was performed as described in Figure 4. Biological replicates are presented. **(B)** C3α'1 and **(C)** C3dg/C3d were significantly elevated in smoke-exposed PBS-treated mice. CR2-fH treatment had little effect, resulting in levels that were mostly indistinguishable from those of PBS controls. Data are expressed as mean ± SEM ($n = 4$ –5 independent samples per condition for protein analysis).

Biodistribution of CR2-fH

We have previously shown that following subretinal injections of AAV5-VMD2-CR2-fH, the presence of the protein can be demonstrated by staining flatmounts of RPE/choroid eyecups with an anti-CR2 antibody or, more quantitatively, using dotblot analysis of retina and RPE/choroid. In our published experiments, we showed that CR2-fH was detectable in both retina and RPE/choroid fractions of mice injected subretinally with AAV5-VMD2-CR2-fH, albeit with higher levels present in the RPE/choroid.³⁵ Here we compared an equal amount of protein for retina and RPE/choroid loaded from animals exposed to AAV5-VMD2-CR2-fH or AAV2-smCBA-CR2-fH. As shown previously, for AAV5-VMD2-CR2-fH-treated animals, most of the CR2-fH protein, 7 months after virus treatment and smoke exposure, was found in the RPE/choroid (Fig. 7A). This polarity is not unexpected since we have shown previously that in eyes of SIOP animals, complement activation products, which would bind and retain CR2-fH, could only be documented by immunohistochemistry in the RPE/BrM/choroid but not in the retina.³⁰ In contrast, in AAV2-smCBA-CR2-fH-treated animals, most of the CR2-fH protein, 7 months after virus treatment and smoke exposure, was found in the retina (Fig. 7A), with very little being extractable from the RPE/choroid.

We have shown previously that CR2-fH delivered via cell encapsulation technology into the vitreous of a mouse can be visualized by immunohistochemistry throughout the retina.³⁵ This observation suggests that while CR2-fH can diffuse throughout the retina, it is not transported across the intact RPE. Here we tested whether CR2-fH delivered to the apical side of an RPE monolayer can be detected on the basal side. ARPE-19 cells were grown as monolayers on Transwell plates for >4 weeks to ensure sufficient barrier formation and lack of paracellular transport.⁴⁷ Then, 10 μg/mL CR2-fH was added to the apical compartment for 4 hours, after which both the apical and basal supernatants were collected. CR2-fH levels were assessed by dotblot analysis. Different amounts of the apical compartment (1, 2.5, 5, and 10 μL)

were loaded when compared to the total volume of the basal compartment (1000 μL). A small amount of CR2-fH (0.5%–1% of the amount added to the apical compartment) could be detected in the basal compartment (Fig. 7B). Martin et al.⁴⁸ have shown that cells can take up full-length fH and that this uptake can be inhibited by the mitochondrial poison NaN₃. To ensure that presence of CR2-fH in the basal compartment is not due to leakage but active transport, the experiment was repeated in the presence of 30 mM NaN₃. Negligible amounts of CR2-fH were detected in the basal compartment after inhibiting ATP-dependent processes (Fig. 7B). Finally, to ensure the intactness of the RPE barrier in the smoke-exposed mouse, the amount of albumin present in the retina was used as a surrogate for blood-retina barrier leakage.⁵⁰ While significant leakage could be demonstrated in animals exposed to laser damage (CNV, samples from previous studies), levels of retinal albumin were indistinguishable between animals exposed to 6 months of smoke or room air (Fig. 7C). Together, these results suggest that RGC transduction leads to the expression of significant amounts of CR2-fH, which, however, does not get across the barrier provided by the RPE, and while a transport mechanism across the RPE does appear to exist for soluble CR2-fH, the effect, which is ATP dependent, appears very inefficient.

DISCUSSION

Complement activation is involved in the pathogenesis of human AMD,^{51,52} which has prompted the search for an anti-complement therapeutic for patients for this very prevalent disease.⁵³ We have used an animal model of dry AMD, the SIOP model, which combines the AMD risk factor of smoking and age (mice are 9–10 months of age by the end of the experiment); it features pathologies commonly seen in AMD (thickening of BrM, deposits, mitochondrial damage) as well as vision loss, and the observed damage is complement dependent.³⁰

The study was driven by asking if long-term delivery of an alternative pathway inhibitor via gene therapy prevents

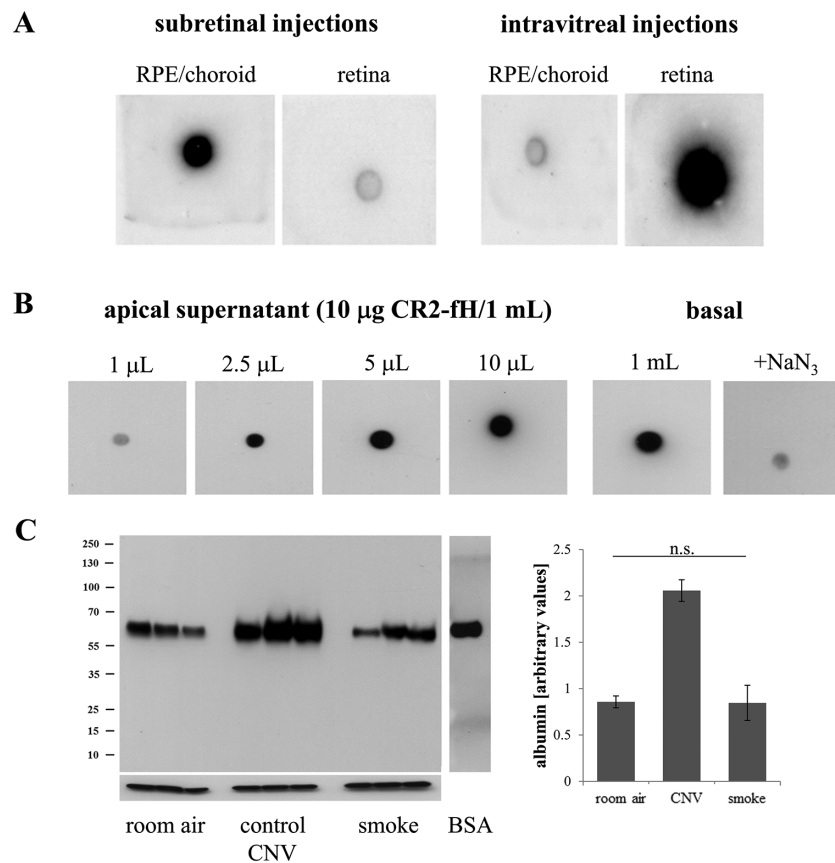


FIGURE 7. Bioavailability of CR2-fH in RPE/choroid. **(A)** Equal amounts of protein (1.5 µg each) per fraction (retina or RPE/choroid) were transferred onto nitrocellulose membranes using the Bio-Dot Microfiltration Apparatus and probed for CR2. Samples from animals injected subretinally versus intravitreally were compared. After subretinal injections, most of the available CR2-positive material was found in the RPE/choroid fraction, whereas in contrast, after intravitreal delivery of the vector, most of the CR2-positive material remained in the retina. **(B)** ARPE-19 cell monolayers grown on Transwell plates were exposed to 10 µg CR2-fH in 1 mL media on the apical side, and apical and basal supernatants (1 mL each) were collected after 4 hours. The entire 1-mL basal supernatant plus four aliquots from the apical (1, 2.5, 5, and 10 µL) supernatant were transferred onto nitrocellulose membranes as described in **(A)** and probed for CR2. A qualitative comparison of the dot intensity suggests that ~0.5% to 1% of the amount added to the apical compartment could be detected in the basal compartment. This transfer of CR2-fH is ATP dependent, since poisoning of mitochondria with NaN₃ significantly reduced the amount of CR2-positive material in the basal compartment. **(C)** To determine leakage of the blood-retina barrier (BRB) after 6 months of smoke exposure, equal amounts of protein (10 µg each) per retina were loaded, separated, and transferred onto nitrocellulose membranes and probed for albumin. Samples from animals raised in room air and smoke were compared, using samples from CNV animals with disrupted BRBs as positive controls ($P < 0.01$ comparing CNV to room air or to smoke). Equal amounts of mouse albumin were found in the retina of SIOP animals when compared to room air controls. Data are expressed as mean \pm SEM normalized to β -actin ($n = 3$ independent samples per condition for protein analysis), and lack of significance is indicated for room air to smoke comparison.

AMD-like pathology in the SIOP model and, if so, whether intravitreally mediated expression can substitute for subretinally mediated delivery. Two specific viral vectors that are optimized for specific tissue targeting were compared: AAV5-VMD2-CR2-fH for delivery to and expression from RPE and AAV2YF-smCBA-CR2-fH optimized for delivery to and expression from cells in the inner retina. The main results are as follows: (1) RPE-mediated secretion of CR2-fH was found to reduce smoke-induced vision loss (contrast threshold), BrM thickening, and mitochondrial swelling; (2) reduction in pathology was correlated with reduced complement activation in RPE/choroid; (3) inner retina-mediated secretion of CR2-fH had no effect on smoke-induced vision loss and minimally affected complement activation in RPE/choroid; and (4) significant levels of CR2-fH are made by either vector. (5) However, bioavailability of CR2-fH in RPE/choroid could only be confirmed after AAV5-VMD2-CR2-fH injection.

(6) Finally, an inefficient, ATP-dependent transport of CR2-fH across the RPE was identified. (7) Hence, our current and previously published data together suggest that in this model, complement activation occurs basal to the RPE (basal RPE, BrM, and choriocapillaris) and hence requires a delivery mechanism that allows for the therapeutic to gain access to this space. And finally, (8) if gene therapy is to be used to treat early AMD, in which the blood-retina barrier is most likely still intact, this argues in favor of AAV vector delivery to the RPE or outside the blood-retina barrier such as the suprachoroidal space.

The Complement Landscape of the Eye

The original focus on complement in the eye of patients with AMD has been the presence of complement activation products in pathologic features of the eye such as drusen and

Bruch's membrane,⁵⁴ as well as the reduction or mislocalization of soluble and membrane-bound complement inhibitors with age and disease progression.⁵⁵⁻⁵⁸ However, it became clear that many of the complement proteins required for activation are not only made by the liver but also by ocular cells.⁵² The RPE and choroid cells express classical pathway and alternative pathway transcripts, including complement C3,⁵² and in iPSC-RPE cells, transcripts for all terminal complement components required to form MAC (C5, C6, C7, C8 γ , and C9) have been reported.⁵⁹

These observations have led researchers to revisit the question as to whether local, systemic, or intracellular complement activation, or all three, are involved in disease pathogenesis. Complement activation products are elevated in patients with disease,⁶⁰ and levels of anaphylatoxins are elevated in both the RPE/choroid and the serum of mice with CNV.⁶¹ However, systemic complement has not been shown to be the driver of disease in patients with liver transplants; the risk of developing AMD is related to the CFH genotype of the recipient.⁶² Likewise, in mice expressing factor B only in the RPE, CNV was indistinguishable from that in wild-type mice.⁶³ Little is known about the potential for intracellular complement activation as a driver of disease. RPE cells have been shown to take up complement components such as C3⁶⁴ and fH⁴⁸ as well as CR2-fH as shown here, and together with the ability of RPE cells to produce complement components, this has led to speculations of intracellular complement activation. In T cells, a novel complement-metabolism-NLRP3 inflammatory axis has been reported that is triggered by intracellular anaphylatoxins.⁶⁵ Of note, in hTERT-RPE1, silencing of fH impaired mitochondrial respiration and glycolysis, altered expression of genes involved in mitophagy and mitochondrial dynamics, and impacted the cells' antioxidant functions.⁶⁶ It will be of great interest to determine whether intracellular CR2-fH can contribute to this noncanonical signaling.

Irrespective of the source of complement, the barrier function of the RPE, together with the diffusion properties of BrM, generates complement compartments. Clark and Bishop¹¹ have shown that BrM acts like a sieve and that larger proteins, especially if glycosylated, cannot permeate. Based on their observations, factor H-like 1, fD, and the anaphylatoxin C5a can diffuse freely across BrM, whereas factor I (fI), fH, fB, and C3a cannot. Hence, there exist four complement compartments that potentially need to be regulated: the retina-apical RPE, the intracellular RPE space itself, the RPE-apical BrM, and the basal BrM-CC compartment, with most complement proteins being synthesized locally in the former three compartments and most derived from the circulation in the latter. This compartmentalization also needs to be kept in mind when designing therapeutics for dry AMD and seems to play a role in interpreting the data obtained here.

CR2-fH Gene Therapy

We have discussed the concept of anticomplement gene therapy in AMD in a previous publication.³⁵ With respect to CR2-fH, we have emphasized the safety and efficacy of the CR2-fH protein. Efficacy was already discussed here earlier. In regards to safety, CR2-fH should not interfere with complement-dependent homeostatic processes; it has a short circulatory half-life in circulation and only binds to

sites of complement activation and not to healthy tissue.⁶⁷ With respect to activity and efficacy, we and others have shown that inhibiting the AP reduces complement activation to homeostatic levels rather than below.^{25,61} Finally, CR2-fH has been shown to provide dose-dependent, linear inhibition of C3 activation, whereas purified full-length fH provided little inhibition, and the CR2 domain alone is ineffective.⁶⁸

Here we examined two approaches to deliver CR2-fH, keeping in mind the complement compartment hypothesis outlined above. Gene therapy delivery to the RPE via subretinal injection for a cytosolic RPE protein has gained US Food and Drug Administration approval for Leber congenital amaurosis type II.⁶⁹ A clinical trial is under way for dry AMD associated with low levels of factor I,⁷⁰ the serine protease that, together with fH, is responsible for the inactivation of C3b. This trial uses subretinal delivery of an AAV vector expressing human complement factor I. It is still unclear, however, whether enough therapeutic protein is produced to affect the area above the injection and what area beyond the injection area might be affected based on product diffusion. Gene delivery to inner retinal cells to date either has been ineffective or has completed the phase I program; AAV2 driving soluble Flt-1 linked to IgG1-Fc using the chicken β -actin promoter failed to reach clinical endpoints for the treatment of wet AMD (NCT01024998),⁷¹ whereas AAV2-mediated expression of sCD59 using the CAG promoter was deemed promising for both the dry (NCT03144999) and wet AMD (NCT03585556).⁷² Here we examined efficacy of AAV5-VMD2-CR2-fH for delivery to RPE and AAV2YF-smCBA-CR2-fH for delivery to inner retinal cells, using optimized AAV serotypes and promoters ensuring cellular specificity. While significant overall production of CR2-fH could be demonstrated for both delivery systems, in the context of an intact blood-retina barrier, most of CR2-fH is retained in the retina upon inner retina-mediated expression, while the majority of CR2-fH is present in the RPE/choroid upon RPE-mediated expression. The molecular weight of CR2-fH is in the range of a Fab fragment. If molecular weight was the main characteristic for transport, in rhesus monkeys, microautoradiography using I¹²⁵-labeled Fab antibody demonstrated that the RPE provides a barrier for the Fab antibody, and Fab antibody was found to be retained in the retina for up to a week, suggesting limited transport across the RPE.⁷³ Knowledge about transport of specific proteins across the RPE, from apical to basal, is limited. Research has focused mostly on photoreceptor outer segment shedding,⁷⁴ as well as exosome⁷⁵ and glutamate uptake,⁷⁶ although C3 uptake by endocytosis⁷⁷ has been reported. Release of material includes the secretion of the RPE secretome,⁷⁸ and exocytosis contributes to the removal of phagocytic residual material at the basolateral plasma membrane if proper lysosomal degradation is inhibited.⁷⁹ Finally, uptake and release of C3H₂O, which results from the slow spontaneous hydrolysis of the internal thioester bond of native C3, has been documented for ARPE-19 cells⁶⁴ as well as uptake of fH,⁴⁸ although polarity was not determined. And while the precise mechanism of transport for CR2-fH across the RPE monolayer is unknown, our data nevertheless suggest that the RPE can transport CR2-fH and probably other proteins from apical to basal in an inefficient, ATP-dependent manner. This limited transport, however, was not sufficient to reduce complement-mediated pathology. Taken together, our data suggest that CR2-fH is a superior AP inhibitor as it inhibits AP activity in a dose-dependent manner, requiring

significantly lower concentrations than endogenous fH, and targets to sites of complement activation. Finally, due to the lack of efficient transport of CR2-fH across the RPE and the requirement for complement inhibition on the basal side of the RPE, we argue in favor of AAV vector delivery to the RPE or outside the blood-retina barrier. Additional studies on CR2-fH diffusion across BrM would complete the argument. While mouse and human BrM share the same pentameric structure, nothing is known about the diffusion characteristics in mouse when compared to human. However, based on its weight (72 kDa), diffusion across human BrM is predicted.¹⁹

We note that there are limitations to this study. The animal model has some similarities to human dry AMD, although the deposits in BrM are in the outer rather than the inner collagenous layer, and the damage is not progressive, such that retinal damage, geographic atrophy, or CNV cannot be examined.³⁰ We have not specifically addressed how complement inhibition reduces BrM thickness and mitochondrial swelling in the RPE, other than to speculate that the mechanism requires inhibition of the complement-oxidative stress feedback loop postulated to be involved in disease.⁸⁰ Smoke has been shown to activate the AP by modifying C3 in a way that reduces its ability to bind to fH.⁸¹ And in RPE culture experiments, we showed that smoke exposure led to oxidative stress, complement activation involving C3a receptor and AP signaling, and endoplasmic reticulum stress and lipid dysregulation, and the vicious cycle could be interrupted and pathology prevented at any level.⁴⁹ And while CR2-fH has been shown to reduce anaphylatoxin generation *in vitro*⁴⁹ and *in vivo*,⁶¹ in the present study, we did not address their role in contributing to pathogenesis. Likewise, any potential effects of CR2-fH on the intracellular milieu of RPE or inner retinal cells have not been investigated. Finally, due to the length and complexity of the study (6 months of daily 5-hour smoke exposure), the study was limited to a single dose and to two delivery modalities. Thus, significantly higher intravitreal doses of the virus, in which intraocular inflammation should be controlled by oral steroid prophylaxis, might provide protection. In addition, new viral vectors that can penetrate the inner limiting membrane⁸² or techniques to enhance AAV delivery to the RPE from the vitreous, such as electric current application,⁸³ should be examined for more safe and efficient gene delivery from the vitreal side.

Acknowledgments

The authors thank Vince Chiodo from the Ophthalmology Vector Core at the University of Florida for the expert help generating the AAV vectors used here and Alfred Lewin from the same institution for critical review of the manuscript.

Supported by the National Institutes of Health (R01EY024581, EY030072), the Department of Veterans Affairs (IK6BX004858, RX000444, and BX003050), and the South Carolina SmartState Endowment at the Medical University of South Carolina (MUSC). In Utah, the following grants are acknowledged: R01 EY015128 (BJ), R01 EY028927 (BJ), P30 EY014800 to Moran Eye Center Core, and Research to Prevent Blindness (New York) Unrestricted Grant to the Department of Ophthalmology & Visual Sciences, University of Utah.

Disclosure: **B. Annamalai**, None; **N. Parsons**, None; **C. Nicholson**, None; **E. Obert**, None; **B. Jones**, None; **B. Rohrer**, CR2-fH technology (P)

References

- Curcio CA. Photoreceptor topography in ageing and age-related maculopathy. *Eye*. 2001;15:376–383.
- Curcio CA, Johnson M. *Structure, Function, and Pathology of Bruch's Membrane*. London, UK: Elsevier; 2013:465–481.
- Bhutto I, Luty G. Understanding age-related macular degeneration (AMD): relationships between the photoreceptor/retinal pigment epithelium/Bruch's membrane/choriocapillaris complex. *Mol Aspects Med*. 2012;33:295–317.
- Terluk MR, Kapphahn RJ, Soukup LM, et al. Investigating mitochondria as a target for treating age-related macular degeneration. *J Neurosci*. 2015;35:7304–7311.
- Ivanova E, Alam NM, Prusky GT, Sagdullaev BT. Blood-retina barrier failure and vision loss in neuron-specific degeneration. *JCI Insight*. 2019;4(8):e126747.
- Sparrow JR, Ueda K, Zhou J. Complement dysregulation in AMD: RPE-Bruch's membrane-choroid. *Mol Aspects Med*. 2012;33:436–445.
- Fearon DT. The complement system and adaptive immunity. *Semin Immunol*. 1998;10:355–361.
- Holers VM. Phenotypes of complement knockouts. *Immunopharmacology*. 2000;49:125–131.
- Muller-Eberhard HJ. Molecular organization and function of the complement system. *Annu Rev Biochem*. 1988;57:321–347.
- Tan PL, Bowes Rickman C, Katsanis N. AMD and the alternative complement pathway: genetics and functional implications. *Hum Genomics*. 2016;10:23.
- Clark SJ, Bishop PN. The eye as a complement dysregulation hotspot. *Semin Immunopathol*. 2018;40:65–74.
- Noris M, Remuzzi G. Overview of complement activation and regulation. *Semin Nephrol*. 2013;33:479–492.
- Liu MM, Chan CC, Tuo J. Genetic mechanisms and age-related macular degeneration: common variants, rare variants, copy number variations, epigenetics, and mitochondrial genetics. *Hum Genomics*. 2012;6:13.
- Yehoshua Z, de Amorim Garcia Filho CA, Nunes RP, et al. Systemic complement inhibition with eculizumab for geographic atrophy in age-related macular degeneration: the complete study. *Ophthalmology*. 2014;121:693–701.
- Taskintuna I, Elsayed ME, Schatz P. Update on clinical trials in dry age-related macular degeneration. *Middle East Afr J Ophthalmol*. 2016;23:13–26.
- Yaspan BL, Williams DF, Holz FG, et al. Targeting factor D of the alternative complement pathway reduces geographic atrophy progression secondary to age-related macular degeneration. *Sci Transl Med*. 2017;9(395):eaff1433.
- Heier JS, Pieramici D, Chakravarthy U, et al. Visual function decline resulting from geographic atrophy: results from the Chroma and Spectri phase 3 trials. *Ophthalmol Retina*. 2020;4(7):673–688.
- Hughes S, Gumas J, Lee R, et al. Prolonged intraocular residence and retinal tissue distribution of a fourth-generation compstatin-based C3 inhibitor in non-human primates. *Clin Immunol*. 2020;214:108391.
- Clark SJ, McHarg S, Tilakaratna V, Brace N, Bishop PN. Bruch's membrane compartmentalizes complement regulation in the eye with implications for therapeutic design in age-related macular degeneration. *Front Immunol*. 2017;8:1778.
- Mullins RF, Dewald AD, Streb LM, Wang K, Kuehn MH, Stone EM. Elevated membrane attack complex in human choroid with high risk complement factor H genotypes. *Exp Eye Res*. 2011;93:565–567.
- Mullins RF, Schoo DP, Sohn EH, et al. The membrane attack complex in aging human choriocapillaris: relationship to macular degeneration and choroidal thinning. *Am J Pathol*. 2014;184:3142–3153.

22. Omri S, Omri B, Savoldelli M, et al. The outer limiting membrane (OLM) revisited: clinical implications. *Clin Ophthalmol*. 2010;4:183–195.
23. Strauss O. The retinal pigment epithelium in visual function. *Physiol Rev*. 2005;85:845–881.
24. Holers VM, Rohrer B, Tomlinson S. CR2-mediated targeting of complement inhibitors: bench-to bedside using a novel strategy for site-specific complement modulation. *Adv Exp Med Biol*. 2013;735:137–154.
25. Alawieh A, Elvington A, Zhu H, et al. Modulation of post-stroke degenerative and regenerative processes and subacute protection by site-targeted inhibition of the alternative pathway of complement. *J Neuroinflammation*. 2015;12:247.
26. Thurman JM, Renner B, Kunchithapautham K, et al. Oxidative stress renders retinal pigment epithelial cells susceptible to complement-mediated injury. *J Biol Chem*. 2009;284:16939–16947.
27. Joseph K, Kulik L, Coughlin B, et al. Oxidative stress sensitizes RPE cells to complement-mediated injury in a natural antibody-, lectin pathway- and phospholipid epitope-dependent manner. *J Biol Chem*. 2013;288(18):12753–12765.
28. Nozaki M, Raisler BJ, Sakurai E, et al. Drusen complement components C3a and C5a promote choroidal neovascularization. *Proc Natl Acad Sci USA*. 2006;103:2328–2333.
29. Campa C, Kasman I, Ye W, Lee WP, Fuh G, Ferrara N. Effects of an anti-VEGF-A monoclonal antibody on laser-induced choroidal neovascularization in mice: optimizing methods to quantify vascular changes. *Invest Ophthalmol Vis Sci*. 2008;49:1178–1183.
30. Woodell A, Coughlin B, Kunchithapautham K, et al. Alternative complement pathway deficiency ameliorates chronic smoke-induced functional and morphological ocular injury. *PLoS ONE*. 2013;8:e67894.
31. Rohrer B, Long Q, Coughlin B, et al. A targeted inhibitor of the alternative complement pathway reduces angiogenesis in a mouse model of age-related macular degeneration. *Invest Ophthalmol Vis Sci*. 2009;50:3056–3064.
32. Woodell A, Jones BW, Williamson T, et al. A targeted inhibitor of the alternative complement pathway accelerates recovery from smoke-induced ocular injury. *Invest Ophthalmol Vis Sci*. 2016;57:1728–1737.
33. Annamalai B, Parsons N, Belhaj M, Brandon C, Potts J, Rohrer B. Encapsulated cell technology-based delivery of a complement inhibitor reduces choroidal neovascularization in a mouse model. *Transl Vis Sci Technol*. 2018;7:3.
34. Annamalai B, Parsons N, Brandon C, Rohrer B. The use of Matrigel combined with encapsulated cell technology to deliver a complement inhibitor in a mouse model of choroidal neovascularization. *Mol Vision*. 2020;26:370–377.
35. Schnabolk G, Parsons N, Obert E, et al. Delivery of CR2-fH using AAV vector therapy as treatment strategy in the mouse model of choroidal neovascularization. *Mol Ther Methods Clin Dev*. 2018;9:1–11.
36. Song H, He C, Knaak C, Guthridge JM, Holers VM, Tomlinson S. Complement receptor 2-mediated targeting of complement inhibitors to sites of complement activation. *J Clin Invest*. 2003;111:1875–1885.
37. Mowat FM, Gornik KR, Dinculescu A, et al. Tyrosine capsid-mutant AAV vectors for gene delivery to the canine retina from a subretinal or intravitreal approach. *Gene Ther*. 2014;21:96–105.
38. Dinculescu A, Glushakova L, Min SH, Hauswirth WW. Adeno-associated virus-vectored gene therapy for retinal disease. *Hum Gene Ther*. 2005;16:649–663.
39. Auricchio A, Kobinger G, Anand V, et al. Exchange of surface proteins impacts on viral vector cellular specificity and transduction characteristics: the retina as a model. *Hum Mol Genet*. 2001;10:3075–3081.
40. Pang JJ, Lauramore A, Deng WT, et al. Comparative analysis of in vivo and in vitro AAV vector transduction in the neonatal mouse retina: effects of serotype and site of administration. *Vision Res*. 2008;48:377–385.
41. Annamalai B, Nicholson C, Parsons N, et al. Immunization against oxidized elastin exacerbates structural and functional damage in mouse model of smoke-induced ocular injury. *Invest Ophthalmol Vis Sci*. 2020;61:45.
42. Anderson JR, Jones BW, Yang JH, et al. A computational framework for ultrastructural mapping of neural circuitry. *PLoS Biol*. 2009;7:e1000074.
43. Stoppelkamp S, Riedel G, Platt B. Culturing conditions determine neuronal and glial excitability. *J Neurosci Methods*. 2010;194:132–138.
44. Leonard AP, Cameron RB, Speiser JL, et al. Quantitative analysis of mitochondrial morphology and membrane potential in living cells using high-content imaging, machine learning, and morphological binning. *Biochim Biophys Acta*. 2015;1853:348–360.
45. Thurman JM, Kulik L, Orth H, et al. Detection of complement activation using monoclonal antibodies against C3d. *J Clin Invest*. 2013;123:2218–2230.
46. Thurman JM, Renner B, Kunchithapautham K, et al. Oxidative stress renders retinal pigment epithelial cells susceptible to complement-mediated injury. *J Biol Chem*. 2009;284:16939–16947.
47. Ablonczy Z, Crosson CE. VEGF modulation of retinal pigment epithelium resistance. *Exp Eye Res*. 2007;85:762–771.
48. Martin M, Leffler J, Smolag KI, et al. Factor H uptake regulates intracellular C3 activation during apoptosis and decreases the inflammatory potential of nucleosomes. *Cell Death Differ*. 2016;23:903–911.
49. Kunchithapautham K, Atkinson C, Rohrer B. Smoke exposure causes endoplasmic reticulum stress and lipid accumulation in retinal pigment epithelium through oxidative stress and complement activation. *J Biol Chem*. 2014;289:14534–14546.
50. Geiger P, Barben M, Grimm C, Samardzija M. Blue light-induced retinal lesions, intraretinal vascular leakage and edema formation in the all-cone mouse retina. *Cell Death Dis*. 2015;6:e1985.
51. Despret DD, Klaver CC, Witteman JC, et al. Complement factor H polymorphism, complement activators, and risk of age-related macular degeneration. *JAMA*. 2006;296:301–309.
52. Anderson DH, Radeke MJ, Gallo NB, et al. The pivotal role of the complement system in aging and age-related macular degeneration: hypothesis re-visited. *Prog Retin Eye Res*. 2010;29:95–112.
53. Kassa E, Ciulla TA, Hussain RM, Dugel PU. Complement inhibition as a therapeutic strategy in retinal disorders. *Expert Opin Biol Ther*. 2019;19:335–342.
54. Hageman GS, Luthert PJ, Victor Chong NH, Johnson LV, Anderson DH, Mullins RF. An integrated hypothesis that considers drusen as biomarkers of immune-mediated processes at the RPE-Bruch's membrane interface in aging and age-related macular degeneration. *Prog Retin Eye Res*. 2001;20:705–732.
55. Fett AL, Hermann MM, Muether PS, Kirchhof B, Fauser S. Immunohistochemical localization of complement regulatory proteins in the human retina. *Histol Histopathol*. 2012;27:357–364.
56. Vogt SD, Curcio CA, Wang L, et al. Retinal pigment epithelial expression of complement regulator CD46 is altered early in the course of geographic atrophy. *Exp Eye Res*. 2011;93:413–423.

57. Ebrahimi KB, Fijalkowski N, Cano M, Handa JT. Decreased membrane complement regulators in the retinal pigmented epithelium contributes to age-related macular degeneration. *J Pathol*. 2013;229:729–742.
58. Yang P, Tyrrell J, Han I, Jaffe GJ. Expression and modulation of RPE cell membrane complement regulatory proteins. *Invest Ophthalmol Vis Sci*. 2009;50:3473–3481.
59. Cerniauskas E, Kurzawa-Akanbi M, Xie L, et al. Complement modulation reverses pathology in Y402H-retinal pigment epithelium cell model of age-related macular degeneration by restoring lysosomal function. *Stem Cells Transl Med*. 2020;9:1585–1603.
60. Heesterbeek TJ, Lechanteur YTE, Lores-Motta L, et al. Complement activation levels are related to disease stage in AMD. *Invest Ophthalmol Vis Sci*. 2020;61:18.
61. Parsons N, Annamalai B, Obert E, Schnabolk G, Tomlinson S, Rohrer B. Inhibition of the alternative complement pathway accelerates repair processes in the murine model of choroidal neovascularization. *Mol Immunol*. 2019;108:8–12.
62. Khandhadia S, Hakobyan S, Heng LZ, et al. Age-related macular degeneration and modification of systemic complement factor H production through liver transplantation. *Ophthalmology*. 2013;120(8):1612–1618.
63. Schnabolk G, Coughlin B, Joseph K, et al. Local production of the alternative pathway component factor B is sufficient to promote laser-induced choroidal neovascularization. *Invest Ophthalmol Vis Sci*. 2015;56:1850–1863.
64. Elvington M, Liszewski MK, Bertram P, Kulkarni HS, Atkinson JP. A C3(H2O) recycling pathway is a component of the intracellular complement system. *J Clin Invest*. 2017;127:970–981.
65. Arbore G, Kemper C. A novel “complement-metabolism-inflammation axis” as a key regulator of immune cell effector function. *Eur J Immunol*. 2016;46:1563–1573.
66. Armento A, Honisch S, Panagiotakopoulou V, et al. Loss of complement factor H impairs antioxidant capacity and energy metabolism of human RPE cells. *Sci Rep*. 2020;10:10320.
67. Alawieh A, Tomlinson S. Injury site-specific targeting of complement inhibitors for treating stroke. *Immunol Rev*. 2016;274:270–280.
68. Huang Y, Qiao F, Atkinson C, Holers VM, Tomlinson S. A novel targeted inhibitor of the alternative pathway of complement and its therapeutic application in ischemia/reperfusion injury. *J Immunol*. 2008;181:8068–8076.
69. Miraldi-Utz V, Coussa RG, Antaki F, Traboulsi EI. Gene therapy for RPE65-related retinal disease. *Ophthalmic Genet*. 2018;39:671–677.
70. Ellis S, Buchberger A, Holder J, Orhane E, Hughes J. GT005, a gene therapy for the treatment of dry age-related macular degeneration (AMD). *Invest Ophthalmol Vis Sci*. 2020;61:2295–2295.
71. Heier JS, Kherani S, Desai S, et al. Intravitreal injection of AAV2-sFLT01 in patients with advanced neovascular age-related macular degeneration: a phase 1, open-label trial. *Lancet*. 2017;390(10089):50–61.
72. Dugel PU. Clinical trial download: data on a gene therapy for dry and wet AMD. *Retinal Physician*. 2020;17:16–17.
73. Mordenti J, Cuthbertson RA, Ferrara N, et al. Comparisons of the intraocular tissue distribution, pharmacokinetics, and safety of 125I-labeled full-length and Fab antibodies in rhesus monkeys following intravitreal administration. *Toxicol Pathol*. 1999;27:536–544.
74. Nandrot EF. Opposite roles of MerTK ligands Gas6 and protein S during retinal phagocytosis. *Adv Exp Med Biol*. 2018;1074:577–583.
75. Shah N, Ishii M, Brandon C, et al. Extracellular vesicle-mediated long-range communication in stressed retinal pigment epithelial cell monolayers. *Biochim Biophys Acta*. 2018;1864:2610–2622.
76. Maenpaa H, Mannerstrom M, Toimela T, Salminen L, Saransaari P, Tahti H. Glutamate uptake is inhibited by tamoxifen and toremifene in cultured retinal pigment epithelial cells. *Pharmacol Toxicol*. 2002;91:116–122.
77. Kaur G, Tan LX, Rathnasamy G, et al. Aberrant early endosome biogenesis mediates complement activation in the retinal pigment epithelium in models of macular degeneration. *Proc Natl Acad Sci USA*. 2018;115:9014–9019.
78. Meyer JG, Garcia TY, Schilling B, Gibson BW, Lamba DA. Proteome and secretome dynamics of human retinal pigment epithelium in response to reactive oxygen species. *Sci Rep*. 2019;9:15440.
79. Peters S, Reinthal E, Blitgen-Heinecke P, Bartz-Schmidt KU, Schraermeyer U. Inhibition of lysosomal degradation in retinal pigment epithelium cells induces exocytosis of phagocytic residual material at the basolateral plasma membrane. *Ophthalmic Res*. 2006;38:83–88.
80. Zarbin MA, Rosenfeld PJ. Pathway-based therapies for age-related macular degeneration: an integrated survey of emerging treatment alternatives. *Retina*. 2010;30:1350–1367.
81. Kew RR, Ghebrehwet B, Janoff A. Cigarette smoke can activate the alternative pathway of complement in vitro by modifying the third component of complement. *J Clin Invest*. 1985;75:1000–1007.
82. Boyd RF, Sledge DG, Boye SL, et al. Photoreceptor-targeted gene delivery using intravitreally administered AAV vectors in dogs. *Gene Ther*. 2016;23:223–230.
83. Song H, Bush RA, Zeng Y, Qian H, Wu Z, Sieving PA. Transocular electric current in vivo enhances AAV-mediated retinal gene transduction after intravitreal vector administration. *Mol Ther Methods Clin Dev*. 2019;13:77–85.